

## Article

# EEG Channel Selection for Stroke Patient Rehabilitation Using BAT Optimizer

Mohammed Azmi Al-Betar <sup>1,\*</sup> , Zaid Abdi Alkareem Alyasseri <sup>2,3,\*</sup> , Noor Kamal Al-Qazzaz <sup>4</sup>,  
Sharif Naser Makhadmeh <sup>1,5</sup> , Nabeel Salih Ali <sup>2</sup>  and Christoph Guger <sup>6</sup> 

- <sup>1</sup> Artificial Intelligence Research Center (AIRC), College of Engineering and Information Technology, Ajman University, Ajman P.O. Box 346, United Arab Emirates; sharif.makhadmeh@uop.edu.jo
- <sup>2</sup> Information Technology Research and Development Center (ITRDC), University of Kufa, Najaf 54001, Iraq; nabeel@uokufa.edu.iq
- <sup>3</sup> College of Engineering, University of Warith Al-Anbiyaa, Karbala 56001, Iraq
- <sup>4</sup> Biomedical Engineering Department, AL-Khwarizmi College of Engineering, University of Baghdad, Baghdad 47146, Iraq; noorbme@kecbu.uobaghdad.edu.iq
- <sup>5</sup> Data Science and Artificial Intelligence Department, Faculty of Information Technology, University of Petra, Amman 1196, Jordan
- <sup>6</sup> G.Tec Medical Engineering GmbH, 4521 Schiedlberg, Austria; guger@gtec.at
- \* Correspondence: m.albetar@ajman.ac.ae (M.A.A.-B.); zaid.alyasseri@uokufa.edu.iq (Z.A.A.A.)

**Abstract:** Stroke is a major cause of mortality worldwide, disrupts cerebral blood flow, leading to severe brain damage. Hemiplegia, a common consequence, results in motor task loss on one side of the body. Many stroke survivors face long-term motor impairments and require great rehabilitation. Electroencephalograms (EEGs) provide a non-invasive method to monitor brain activity and have been used in brain–computer interfaces (BCIs) to help in rehabilitation. Motor imagery (MI) tasks, detected through EEG, are pivotal for developing BCIs that assist patients in regaining motor purpose. However, interpreting EEG signals for MI tasks remains challenging due to their complexity and low signal-to-noise ratio. The main aim of this study is to focus on optimizing channel selection in EEG-based BCIs specifically for stroke rehabilitation. Determining the most informative EEG channels is crucial for capturing the neural signals related to motor impairments in stroke patients. In this paper, a binary bat algorithm (BA)-based optimization method is proposed to select the most relevant channels tailored to the unique neurophysiological changes in stroke patients. This approach is able to enhance the BCI performance by improving classification accuracy and reducing data dimensionality. We use time–entropy–frequency (TEF) attributes, processed through automated independent component analysis with wavelet transform (AICA-WT) denoising, to enhance signal clarity. The selected channels and features are proved through a k-nearest neighbor (KNN) classifier using public BCI datasets, demonstrating improved classification of MI tasks and the potential for better rehabilitation outcomes.

**Keywords:** EEG; feature extraction; channel selection; stroke patients; BAT algorithm



**Citation:** Al-Betar, M.A.; Alyasseri, Z.A.A.; Al-Qazzaz, N.K.; Makhadmeh, S.N.; Ali, N.S.; Guger, C. EEG Channel Selection for Stroke Patient Rehabilitation Using BAT Optimizer. *Algorithms* **2024**, *17*, 346. <https://doi.org/10.3390/a17080346>

Academic Editor: Gabriella Trucco

Received: 21 May 2024

Revised: 14 July 2024

Accepted: 15 July 2024

Published: 8 August 2024



**Copyright:** © 2024 by the authors. Licensee MDPI, Basel, Switzerland. This article is an open access article distributed under the terms and conditions of the Creative Commons Attribution (CC BY) license (<https://creativecommons.org/licenses/by/4.0/>).

## 1. Introduction

The World Health Organization (WHO) lists stroke as the second greatest cause of mortality globally because of the damage it causes to the brain through disruptions in cerebral circulation [1,2]. One of the most debilitating forms of nervous system damage is hemiplegia, which describes partial or complete paralysis of one side of the body including the arm, leg, foot, and hand. Ischemic stroke, the most common type of stroke, causes interruption of cerebral perfusion, which results in rapid loss of brain function [3,4]. Sixty percent or more of stroke survivors require rehabilitation due to permanent motor function impairment [5]. However, stroke survivors endure a wide range of disabilities, including visual and cognitive deficits, that have a cumulatively devastating effect on their ability to

carry out even the most basic of tasks. Accordingly, research into efficient treatment and rehabilitation of stroke victims has been a focus for many years [6].

An electroencephalogram (EEG) is a non-invasive method that estimates the electrical activity of the brain with good time resolution in order to define the results of a variety of mental tasks. By translating brain EEG signals into control instructions, brain-computer interfaces (BCIs) help people with physical impairments interact with the sensory world outside [7]. Motor imagery (MI) is the mental imagining of body movement without real muscle movement, and its accompanying rhythmic activities of the brain can be recorded and used as the input signals of BCI systems. Event-related desynchronization/synchronization (ERD/ERS) refers to the detection of the rhythmic power changes in the sensorimotor area within the Rolandic mu (9–13 Hz) and beta (13–30 Hz) frequency bands, which can be used to distinguish between various types of MI tasks [8]. Due to the fact that MI does not require any extraneous stimuli, BCIs based on MI have a wide variety of potential uses [9].

The volatility and complexity of EEG signals, however, cause difficulties for conventional MI-BCI decoding [7]. Crucial and difficult issues remain in enhancing EEG decoding capacity, extracting discriminative information from low signal-to-noise EEGs, and realizing reliable classification of various MI tasks [8].

Channel selection in EEG-based investigations is important to determine the subset of channels that is most informative in terms of capturing the proper neural signals for the chosen application [10]. Nevertheless, such considerations and their corresponding challenges may differ in other application contexts, and that can be seen when comparing stroke rehabilitation with emotion processing and dementia detection using an EEG-based dataset [11]. For example, stroke rehabilitation is characterized by the fact that with neurological defects resulting from the stroke event, there are certain modifications in the activity of the brain and the functioning of the neural networks. EEG data can also be characterized by specific features that distinguish them from healthy subjects or other patients, such as changes in the topological organization of networks, aberrant activity, and appearance of novel regulatory strategies [12].

Therefore, the approach to choosing the most significant EEG channels for stroke rehabilitation may need to be more selective and specific. The idea is to find out which of the channels provides the best recording of the neural characteristics of the particular motor, cognitive, or behavioral impairment which a stroke patient may present, and it will not be the same as the channels that would be ideal for other applications [13]. However, there are distinct approaches such as emotion processing and dementia detection that may employ different neurophysiological mechanisms and/or spectrotemporal patterns. For example, in emotion processing, the frequency band related to emotion processing can be spread across different cortical areas, and the aim of the channel selection could be to capture this distributed frequency activity. Similarly, in the case of dementia detection, the alteration of brain structure and function which define cognitive impairment might represent a different spatial distribution of load that calls for different rules for choosing the channels [14]. With a direct focus on the channel selection problem in the context of stroke rehabilitation, the proposed study intends to contribute an effective solution that can improve the performance of a BCI and thus improve the rehabilitation process.

Channel selection is the main focus of this study. Many electrodes are utilized in medical and diagnostic treatments. For practical BCI applications, many electrodes are needed for classification accuracy; however, putting many electrodes on the scalp is time-consuming and subject to EEG signal overfitting. To fix these issues, researchers need to identify the electrodes that are unable to be classified. Electrode selection can evaluate the neurological knowledge of individuals due to varying reactions and subject-dependent ideal electrode placement [15]. The user-dependent classification job requires automatic electrode relevance determination. This challenge can be overcome by considering a wide range of electrodes and using many methods to identify the appropriate channels for each patient. A particle BA-based optimization technique was used to pick the most accurate

EEG channels for stroke patient rehabilitation. Each EEG data channel provides unique classification features. Channel selection reduces data storage and processing, speeds up classifier training by using simpler data, and reduces the “curse of dimensionality”.

Many studies have examined channel selection in healthy people [16,17], whereas the present study focuses on stroke rehabilitation, where stroke patients’ underlying neurophysiological abnormalities and limitations may demand a customized channel selection strategy.

Choosing EEG channels for emotion processing, cognitive assessment, and clinical diagnosis often involves knowledge of neural mechanisms and brain regions linked with the desired activities. Common brain activity patterns and optimal channel selection are well established for healthy people. However, strokes can alter brain structure, connectivity, and function. These alterations may cause abnormal brain patterns and compensatory processes [18,19]. Thus, the best EEG channels for stroke rehabilitation may differ from those recommended for healthy people.

To capture stroke patients’ neural correlates of motor, cognitive, and behavioral abnormalities, channel selection must be more specialized and personalized due to stroke-induced neuroplasticity. Targeting stroke patients with a customized solution that can properly recognize neural fingerprints and brain activity patterns is intended to connect stroke-related deficiencies. This stage is crucial to developing BCI-based stroke therapies that improve rehabilitation outcomes [20].

The literature on channel selection in healthy people can be useful, but this study recognizes the need to address stroke survivors’ unique issues and considerations. Scientists examined channel selection differences between stroke patients and healthy people to better understand neurophysiological changes and optimal BCI setups for stroke rehabilitation.

Therefore, in this study, a binary bat algorithm (BA)-based optimization method is used to identify the most important EEG channels for stroke rehabilitation. Thus, this method is suited to stroke survivors’ needs by optimizing BCI technology and rehabilitation effectiveness.

Raw EEG data are segmented and filtered using standard filters and the automated independent component analysis with wavelet transform (AICA-WT) denoising approach in an effort to address the issues mentioned above. Then, time–entropy–frequency (TEF) attributes are created by combining the effective features from the time, entropy, and frequency domains. As a result, the BA-based optimization method is used to optimize the TEF characteristics in order to choose the efficient channels that improve the stationarity and resilience of the system. After we train a KNN classifier technique, we conduct a series of experiments to evaluate our proposed framework using 25 MI-based BCI sessions with follow-up assessment visits to examine the functional changes before and after EEG neurorehabilitation from public datasets from the BCI Competition. The hybrid time–entropy–frequency (TEF) attributes used in the AICA-WT-TEF-Chs framework for MI-BCI classification are intended to efficiently leverage the underlying information of the time, entropy, and frequency domains on classification performance.

The approach suggested in this paper makes the following contributions. First, it looks at how time–entropy–frequency (TEF) variables affect classification performance. Second, it uses the effective EEG channels generated by a BA-based optimization method to detect changes both before and after rehabilitation. Third, it tests the effectiveness of the AICA-WT-TEF-Chs framework utilizing a variety of classification models and cutting-edge techniques. By eliminating extraneous dimensions, effective channel selection decreases the amount of data that must be stored and processed, speeds up classifier training by using simpler data, and prevents classifier overfitting by lessening the impact of the “curse of dimensionality”.

## 2. Related Works

EEG-based BCIs in particular have good temporal resolution [21], but the recorded wave activity may be corrupted in a variety of ways depending on the artifacts that occurred, so preprocessing the raw EEG signals is critical in the classification of MI-based signals.

Most of the time, these artifacts can imitate or overlay the abnormal behavior of the brain. Studies have investigated artifacts' effects on EEG signals, including eye blinks, ocular movements, cardiac artifacts, and muscular activity, and noise from power lines can also intersect an EEG's frequencies [22,23]. As a result, assessing the efficiency of EEG signals in the presence of background noise can be difficult. Spatial filters can produce a more localized signal for each electrode in this situation because EEG-based BCIs in particular have poor spatial resolution.

To choose the best characteristics for BCI-MI-based EEG analysis, feature extraction is carried out for each recorded channel in multiple domains. The most popular technique is to use common spatial patterns (CSPs) to obtain discriminant features from high-dimensional EEG signals, which may be used to identify the spatial characteristics related to ERD produced by various MI tasks [24]. However, the efficiency of CSPs is easily impacted by noise and is highly sensitive to the choice of frequency bands [16]. Several feature extraction techniques were developed to analyze the EEG data in the time, frequency, and time-frequency domains to address the issue of efficacy [25]. Additionally, wavelet coherence (WC) bispectrum characteristics were suggested in [26] for distinguishing between right and left MI.

The sizes of the features derived from EEG signals are usually pretty big for each channel, and they get bigger when one moves to the next channel. The classification of several features necessitates additional computation and time. To solve this issue, the most effective feature set must be obtained by selecting a subset of EEG channels that are more closely related to mental work than others. The four evaluation methodologies of filtering, wrapping, embedding, and hybrid can be used to categorize feature selection algorithms [27]. Based on specific statistical criteria, the filtering method used for motor intention-based EEG activities is taken into consideration. For instance, before classifying the motor intent activity, He et al. [28] developed the statistical method of the Bhattacharyya bound for channel selection. The best candidate subset was chosen using this method, which also employed a CSP and sequential search strategy. Tam et al. [29] suggested a different statistical method based on CSP rank for sorting filter coefficients with absolute values and then choosing the features with the biggest succeeding coefficient. Although the filtering technique has low accuracy, it operates quickly and is unaffected by the subject or classifier choice.

On the other hand, the classifier and the subject are quite important in the wrapper selection process [30]. In this way, the subset candidates are assessed using classification accuracy and can thus make more accurate predictions than filtering techniques. As a result, the wrapper strategy is more computationally expensive than the filtering technique and is subject to the overfitting problem [31], which can be avoided by employing cross-validation measures for prediction. For choosing the best channel, the majority of wrapper strategies use the sequential forward search, backward elimination strategy [32], and heuristic search method [33,34]. Without mentioning a stopping condition, the filtering and wrapping procedures have also been coupled for selection purposes. This hybrid strategy was created to deal with huge datasets. Gaur et al., for instance [35], offered the best possible channel selection technique based on CSPs. Before ranking all the channels according to their scores and using the classification accuracy to evaluate the chosen ideal channel combination, they first applied the L1 norm of a CSP to group the channel contribution scores. Finally, using the defined criteria for a particular classifier's learning process, the embedded approach was used to choose significant channels.

To choose channels with the best classification outcomes, Shi et al. [36] used feature selection techniques, recursive feature removal, and zero-norm optimization trained with support vector machines. The use of these techniques allowed the EEG channels to be significantly reduced [37].

The crucial step in the classification of EEG data is to use pertinent features that significantly affect the system's ability to classify data effectively [38–40]. Therefore, to achieve the best classification performance, it is necessary to use valid features from EEG signals [41].

Furthermore, global optimization techniques and machine learning classification can be combined to address such problems in the BCI domain, including feature extraction and selection [42]. Several algorithms gained a lot of interest for their applications in feature selection, for instance, differential evolution (DE), simulated annealing (SA), particle swarm optimization (PSO), artificial bee colony (ABC), and ant colony optimization (ACO) [43].

Research has been conducted on channel selection for different BCI paradigms including recursive channel elimination for motor imagery tasks [44]. In a study that was conducted by Rakotomamonjy et al. [45], the researchers used a channel selection technique that was built into the training of an SVM classifier. The space of features was searched using GA in the references [46,47], and the fitness function was the weighted linear combination of the number of features and the accuracy of the SVM. Udhaya et al. in [48] suggested a PSO-based rough set feature selection approach to determine the best subset of features, and the accuracy of a neighborhood classifier was utilized as the evaluation criterion for the feature subset. DE was utilized by Baig et al. [49], and PSO and GA were utilized by Atyabi et al. [50] in order to find the best feature subset, respectively. In [51], the process of selecting characteristics for EEG-based emotion identification used ant colony optimization, simulated annealing, genetic algorithms, particle swarm optimization, and differential evolution. The performance of these EA-based approaches for feature selection is quite encouraging.

However, the size of the search area is predetermined in these algorithms; therefore, throughout each iteration, it is important to make a decision regarding whether or not each feature should be chosen. Under these circumstances, the computational effort will be wasted on some features that are superfluous, unnecessary, or of a trivial nature. In addition, evolutionary algorithms (EAs) readily converge to a local optimum as a result of the wide search space as well as the interference of redundant, irrelevant, and trivial features. In this study, we design EA-based feature selection methods for motor imagery BCI through the reduction of dimensionality.

The performance of a classifier will dramatically decline as the number of features increases due to the dimensionality curse, which occurs when the number of features surpasses a specific threshold. Additionally, the training procedure takes longer the higher the feature dimensionality becomes [46].

In order to locate a large number of existing channels, feature selection is required with a thorough search for extracting related channels [10,52]. Researchers have focused on feature selection issues and suggested complete search-, greedy search-, and random search-based approaches [11]. High computational costs and convergence to local optimum remain issues with these selection techniques [53].

### 3. BAT Algorithm

In this section, the bat optimization algorithm is introduced and illustrated in terms of its inspiration, microbats, and their lifestyle in nature, along with the method's general optimization procedure and mathematical formulation.

#### 3.1. Inspiration of BAT

The bat optimization algorithm was first proposed by Xin-She Yang in 2010 [54]. Xin-She Yang proposed the bat algorithm based on microbats' characteristics of echolocation, used for hunting prey, and movement in darkness. A microbat produces extremely loud sound pulses and hears their echo from the objects and prey around it. Based on the echo sound, bats can define the type of prey and the strategy for hunting it. The bats usually produce 10 to 20 pulses every second when they are searching for prey. Once they are close to the prey, the number of pulses increases to 200 pulses every second and the sound pulse becomes quieter.

In nature, microbats have a collective hunting behavior, where they fly together with determined velocity to hunt prey simultaneously by using the echolocation characteristic, as shown in Figure 1. The figure presents the movement of microbats based on the echoloca-

tion mechanism, where the microbats update their locations and move toward prey based on the echo sound and the location of other microbats, determined by interacting with each other. Furthermore, the microbats' velocity becomes higher and the pulses lower when the microbats are close to the prey location.

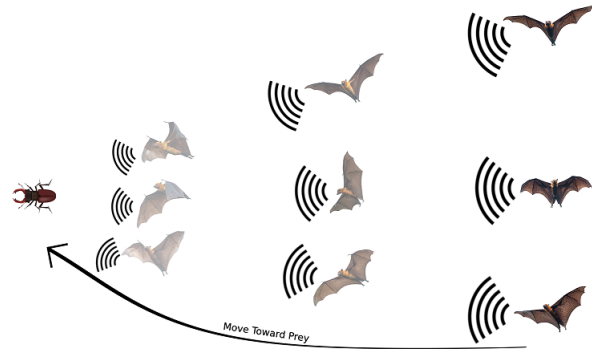


Figure 1. Bat movement toward prey.

In the BAT algorithm, each microbat is considered as a solution in the population, the position of the prey is the optimal solution for a particular optimization problem, the location is presented in a vector  $x$  with a range between  $f_{min}$  and  $f_{max}$ , the velocity of microbats is presented in a vector  $v$ , and the wavelength is  $\lambda$  with pulse rate  $r \in [0, 1]$  and loudness range  $A$ , where the largest is presented as  $A_0$  and the lowest is  $A_{min}$ .

3.2. Procedure of BAT

This section presents the general optimization procedure of the BAT algorithm. This optimization procedure contains six main steps, which are presented in Figure 2 and thoroughly discussed below:

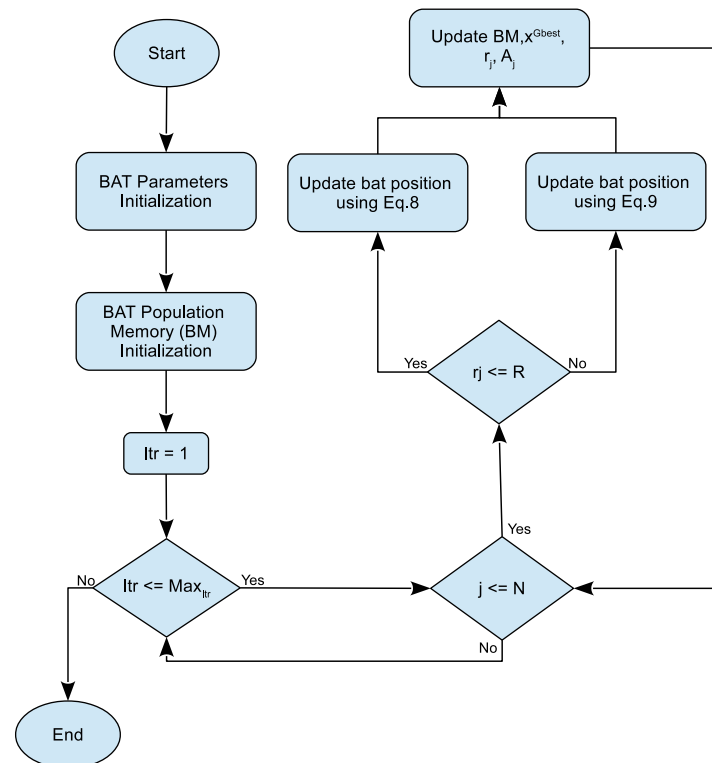


Figure 2. Bat algorithm flowchart.

- Step 1: BAT algorithm parameter initialization. In this step, the BAT parameters are initialized with initial values. These parameters are the number of microbats

(solutions) ( $N$ ), maximum number of iterations ( $Max_{Iter}$ ),  $\max(f_{max})$  and  $\min(f_{min})$  frequency range, velocity vector ( $v$ ), loudness rate ( $A$ ), pulse rate ( $r$ ), initial pulse rate ( $r^0$ ), two parameters ( $\lambda$  and  $\alpha$ ) with constant values in the range  $[0, 1]$ , and bandwidth range ( $\epsilon$ ) in the range  $[-1, 1]$ .

- Step 2: BAT population memory initialization. The BAT solutions are randomly generated in this step using Equation (1), considering the BAT algorithm and particular optimization problem parameters and constraints.

$$x_i^j = lb_i + (ub_i - lb_i) \times R, \tag{1}$$

where  $\forall i = 1, 2, \dots, d, \forall j = 1, 2, \dots, N$ , and  $R$  is a random number between 0 and 1. The produced solutions together generate the population, as shown in Equation (2), and are stored in the BAT memory (BM) in ascending order on the basis of their fitness values. The best solution with the fittest values is assigned to  $x^{Gbest}$  and stored in the first position of the BM.

$$BM = \begin{bmatrix} x_1^1 & x_2^1 & \dots & x_d^1 \\ x_1^2 & x_2^2 & \dots & x_d^2 \\ \vdots & \vdots & \dots & \vdots \\ x_1^N & x_2^N & \dots & x_d^N \end{bmatrix}, \tag{2}$$

- Step 3: Bat population intensification. Now, all microbats  $x$  fly and change their position considering a velocity  $v$  defined by a frequency  $f$  that is generated randomly, as shown in Equations (3) and (4). Accordingly, the bat positions are updated using Equation (5).

$$f_i = f_{min} + (f_{min} - f_{max}) \times R, \tag{3}$$

$$v_i^j = v_i^j + (x_i^j - x^{Gbest}) \times f_i, \tag{4}$$

$$x_i^j = x_i^j + v_i^j, \tag{5}$$

It is notable that the microbats update their locations to be closer to the global best ( $x^{Gbest}$ ). Thus, the new position of the microbats intensifies the position in a direction toward  $x^{Gbest}$ .

- Step 4: Bat population diversification. In this step, the microbats' positions are updated based on random parameters to attempt to find better global solutions. A new solution is selected from the BM based on a selection method and assigned to  $x^{Gbest}$ . Subsequently, the current solution is updated using  $x^{Gbest}$  as follows:

$$x_i^j = x^{Gbest} + \epsilon \times A_j', \tag{6}$$

where  $A'$  is the loudness average. As Steps 3 and 4 are contradictory steps, the BAT algorithm chooses one of them at a time for execution. This selection is based on the following equation:

$$x^j = \begin{cases} x^{Gbest} + \epsilon \times A_j' & \text{if } r_j \leq R \\ x^j + v^j & \text{otherwise} \end{cases}, \tag{7}$$

- Step 5: BM update. The position of the microbats in the BM will be updated in this step if the new location is fitter than the old one and  $R \leq A_j$ . Moreover,  $x^{Gbest}$  will be

updated if the new BM contains a solution with a better fitness value. Subsequently,  $r_j$  and  $A_j$  values will be updated in accordance with Equations (8) and (9).

$$r_j = r_j^0(1 - e^{(-\gamma \times itr)}), \tag{8}$$

$$A_j = \alpha \times A_j, \tag{9}$$

where  $itr$  denotes the current iteration number.

- Step 6: Stop criterion. Steps 3, 4, and 5 will be repeated until the algorithm reaches the stop criterion.

### 4. Proposed Method

This section presents the main contribution of this paper. The proposed method includes five phases, which are presented in Figure 3 and thoroughly discussed below.

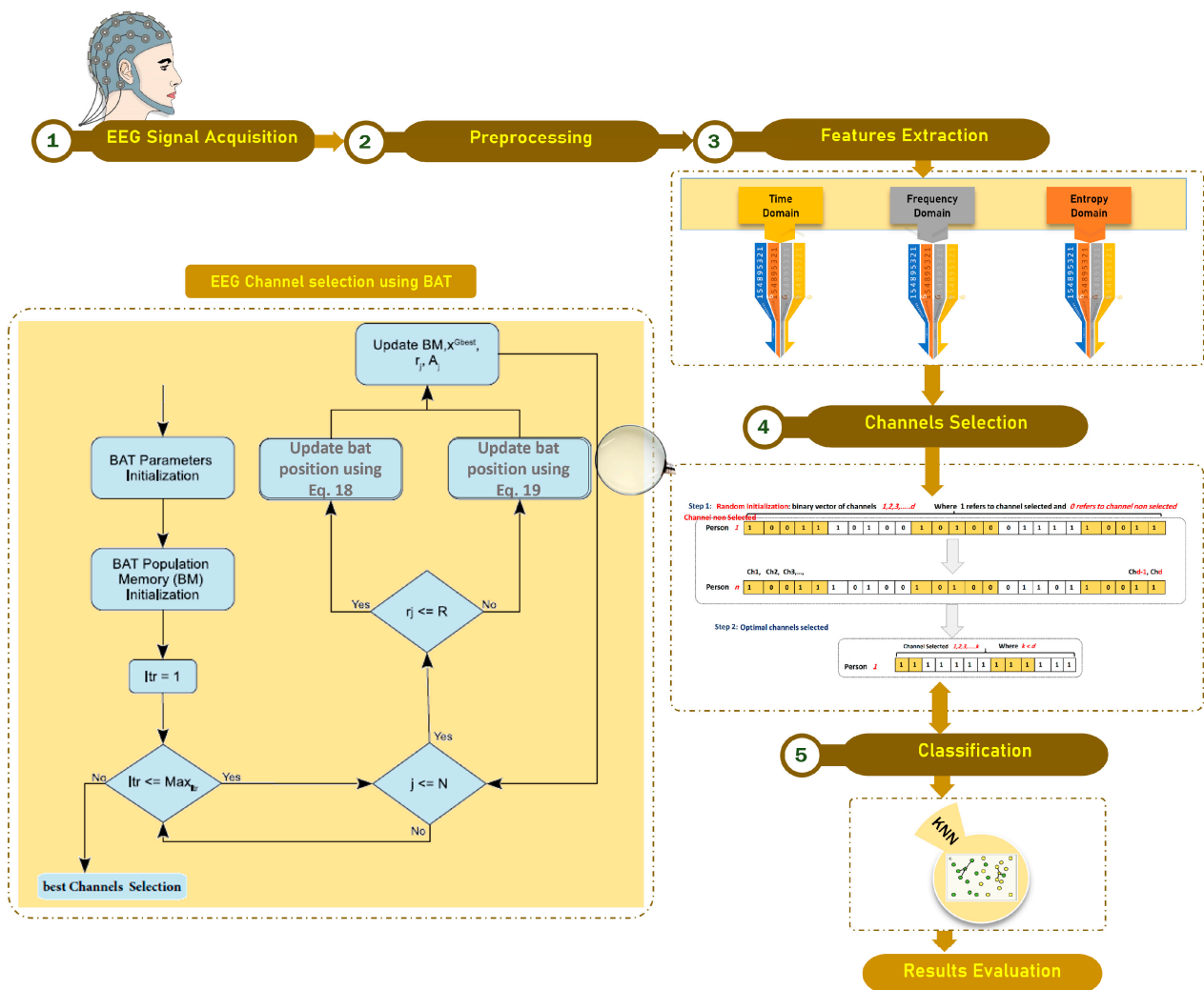
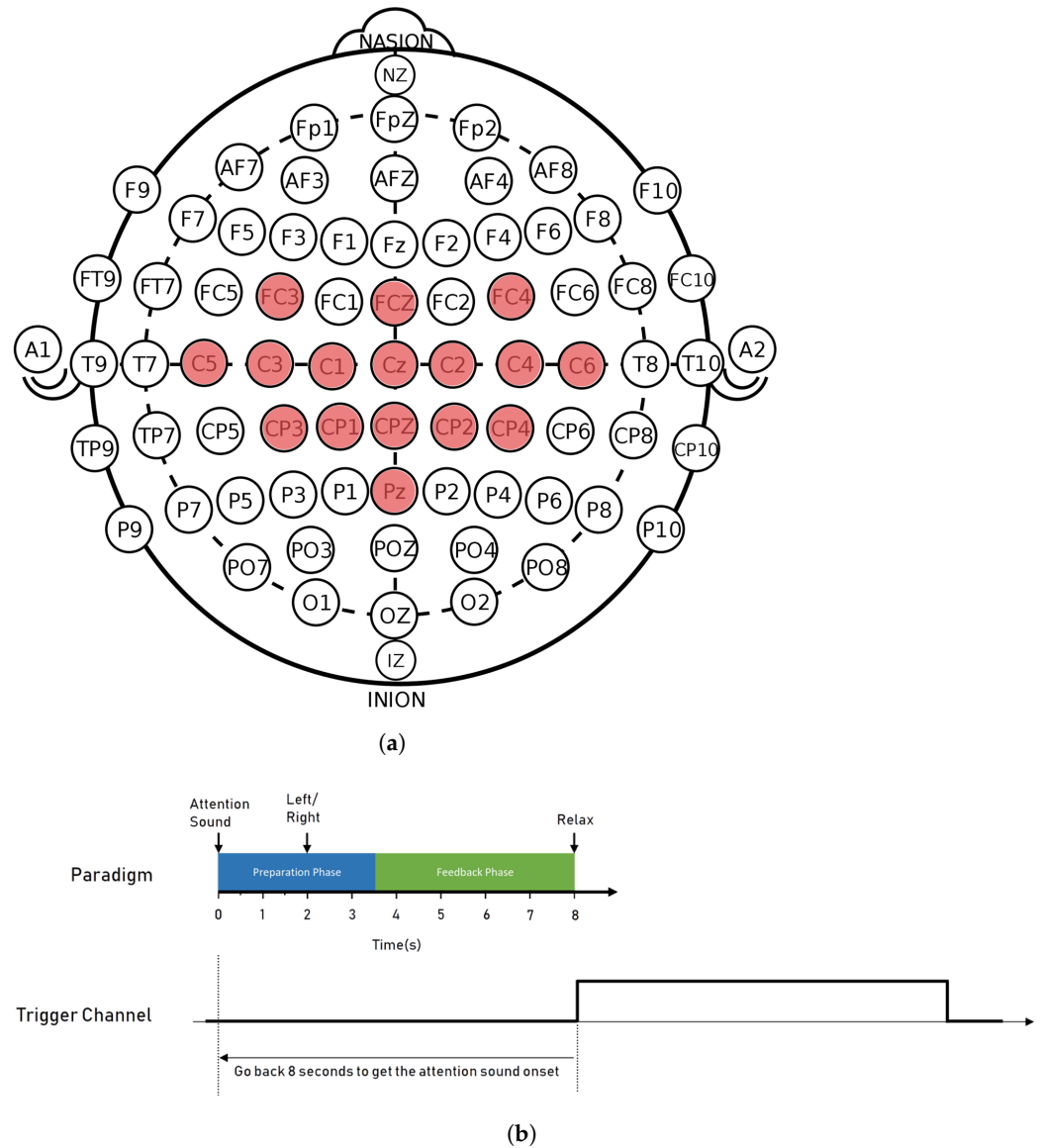


Figure 3. A proposed method for electroencephalogram channel selection.

#### 4.1. Phase I: EEG Signal Acquisition

In this study, the source of the dataset is from g.tec Medical Engineering GmbH, a standard EEG dataset; details about this dataset are explained in [8]. The EEG data of poststroke patients with hemiparesis of the upper extremities were studied. This study involved 8 poststroke patients treated with the recoveriX system (g.tec medical engineering

GmbH), with a mean age of 22 years ( $SD = 4.582$ ). Each participant received BCI-based MI training for three months, with 2 training sessions each week (for a total of 25 training sessions). The study team conducted and analyzed two assessments (pre- and post-training). The pretraining evaluation was scheduled 30 to 35 days prior to the intervention, and the post-training evaluation was conducted a few days after the intervention (see Figure 4). The Ethikkommission des Landes Oberosterreich in Austria (#D-42-17) authorized this study protocol, and each patient signed an informed consent form prior to the preassessment. Finally, this dataset is captured with a sample rate of 256 Hz.



**Figure 4.** (a) EEG electrode distributions based on 10–20 system; (b) schematic diagram of EEG recording protocol.

According to system indications for an MI mental task, the patients were instructed to visualize dorsal wrist movement. Prior to and after EEG neurorehabilitation, the patients participated in 25 MI-based BCI sessions with follow-up evaluation visits to measure the functional changes. Each session consisted of 240 MI repetitions with both hands, broken down into three 80-trial runs. Each session lasted approximately one hour, including the time required for setup and cleanup. The MI-based BCI tasks were illustrated with randomized inter-trial intervals in a pseudo-random order.

For capturing all the various neural processes that take place during stroke rehabilitation—involving cognitive, affective, and motor components—sixteen-channel active EEG caps were employed. The caps were made by the g.tec medical engineering GmbH company in Austria.

According to the international 10–20 system, the EEG electrodes were positioned as follows: (FC5, FC1, FCz, FC2, FC6, C5, C3, C1, Cz, C2, C4, C6, CP5, CP1, CP2, and CP6). To the subject, a ground electrode was applied at FPz and a reference electrode was affixed at the right earlobe.

These channels are linked with different cognitive and sensorimotor processes which are in some way impaired in patients after a stroke. Particularly, the frontocentral channels (FC5, FC1, FCz, FC2, FC6) are associated with emotional regulation, working memory, and secondary motor area. Further, it is important to note that the central channels (C5, C3, C1, Cz, C2, C4, and C6) are related to sensory–motor integration and body movement representation. In addition, the centroparietal channels (CP5, CP1, CP2, CP6) are described to be involved in the process of integration of the exteroceptive and the proprioceptive inputs as well as in the regulation of the voluntary movements [22].

#### 4.2. Phase II: Preprocessing

Each channel of the recorded EEG dataset initially used two standard filters. First, a bandpass filter (BPF) with frequencies between (8 and 30 Hz) was used to confine the band of the recorded EEG data, and second, a Butterworth (BW) notch filter at (50 Hz) was used to reduce the noise from power line interference. (ICs)  $s(t) = [s_1(t), \dots, s_n(t)]$ , utilizing the *FastICA* algorithm proposed by [55]. The set  $s(t)$  of  $n$  unknown components that were linearly mixed within matrix  $A$  and the set  $x(t)$  of  $n$  observations where  $x(t) = [x_1(t), \dots, x_n(t)]$  [56–58] represent the EEGs and are related to  $s(t)$ ,  $t$ , which is the time; hence, the ICA equation is

$$x(t) = As(t) \quad (10)$$

Then, three metrics were used to evaluate the artifactual components, ICs: kurtosis (*Kurt*), skewness (*Skw*), and sample entropy (*SampEn*). If these parameters surpassed the  $pm1.2$  threshold for each IC, the IC was marked as critical and denoised using WT. The practical value of the threshold was determined through trial and error and previous research [59–61]. The threshold value of  $\pm 1.2$  is not a drawback of the AICA–WT technique, as the artifactual ICs were not rejected but were denoised using the WT technique. As a result, WT denoised the marked ICs before returning the enhanced components to the original EEG dataset [22,23].

#### 4.3. Phase III: EEG Feature Extraction

Three different feature extraction techniques are used in this work. These techniques include time domain features, entropy features, and frequency domain features as extracted in [8].

#### 4.4. Phase IV: EEG Channel Selection Using BAT Optimizer

This phase is the main contribution, and it includes several steps to achieve the optimal subset of the EEG channels which can provide the highest accuracy rate. The following steps represent how we adapt the BAT optimizer for the EEG channel selection problem:

- Step 1: BAT algorithm parameter initialization. In this step, the BAT parameters are initialized with initial values. These parameters are the number of microbats (solutions) ( $N$ ), maximum number of iterations ( $Max_{Itr}$ ), max ( $f_{max}$ ) and min ( $f_{min}$ ) frequency range, velocity vector ( $v$ ), loudness rate ( $A$ ), pulse rate ( $r$ ), initial pulse rate ( $r^0$ ), two parameters ( $\lambda$  and  $\alpha$ ) with constant values in the range  $[0, 1]$ , and bandwidth range ( $\epsilon$ ) in the range  $[-1, 1]$ , as shown in Table 1.

**Table 1.** Metaheuristic parameters.

Algorithm	Parameters	Population Size	Runs
CS	$\beta = 1.5, P_a = 0.25$	20	30
PSO	$c1 = c2 = 2$	20	30
BAT	$A = 0.5, r = 0.5$	20	30
FFA	$\alpha = 0.5, \gamma = 1, \beta_0 = 0.2$	20	30
GWO	-	20	30

- Step 2: BAT population memory initialization. The BAT solutions are randomly generated in this step using Equation (11), considering the BAT algorithm and particular optimization problem parameters and constraints.

$$x_i^j = lb_i + (ub_i - lb_i) \times R, \tag{11}$$

where  $\forall i = 1, 2, \dots, d, \forall j = 1, 2, \dots, N$ , and  $R$  is a random number between 0 and 1. The produced solutions together generate the population, as shown in Equation (12), and are stored in the BAT memory (BM) in ascending order on the basis of their fitness values. The best solution with the fittest values is assigned to  $x^{Gbest}$  and stored in the first position of the BM.

$$BM = \begin{bmatrix} x_1^1 & x_2^1 & \dots & x_d^1 \\ x_1^2 & x_2^2 & \dots & x_d^2 \\ \vdots & \vdots & \dots & \vdots \\ x_1^N & x_2^N & \dots & x_d^N \end{bmatrix}, \tag{12}$$

- Step 3: BAT population intensification. Now, all microbats  $x$  fly and change their position considering a velocity  $v$  defined by a frequency  $f$  that is generated randomly, as shown in Equations (13) and (14). Accordingly, the bat positions are updated using Equation (15).

$$f_i = f_{min} + (f_{min} - f_{max}) \times R, \tag{13}$$

$$v_i^j = v_i^j + (x_i^j - x_i^{Gbest}) \times f_i, \tag{14}$$

$$x_i^j = x_i^j + v_i^j, \tag{15}$$

It is notable that the microbats update their locations to be closer to the global best ( $x^{Gbest}$ ). Thus, the new position of the microbats intensifies the position in a direction towards  $x^{Gbest}$ .

- Step 4: BAT population diversification. In this step, the microbats' positions are updated based on random parameters to attempt to find better global solutions. A new solution is selected from the BM based on a selection method and assigned to  $x^{best}$ . Subsequently, the current solution is updated using  $x^{best}$ , as follows:

$$x_i^j = x^{best} + \varepsilon \times A'_j, \tag{16}$$

where  $A'$  is the loudness average. As Steps 3 and 4 are contradictory steps, the BAT algorithm chooses one of them at a time for execution. This selection is based on the following equation:

$$x^j = \begin{cases} x^{best} + \varepsilon \times A'_j & \text{if } r_j \leq R \\ x^j + v^j & \text{otherwise} \end{cases}, \tag{17}$$

- Step 5: BM update. The position of the microbats in the BM will be updated in this step if the new location is fitter than the old one and  $R \leq A_j$ . Moreover,  $X^{G_{best}}$  will be updated if the new BM contains a solution with a better fitness value. Subsequently,  $r_j$  and  $A_j$  values will be updated in accordance with Equations (18) and (19).

$$r_j = r_j^0(1 - e^{(-\gamma \times itr)}), \quad (18)$$

$$A_j = \alpha \times A_j, \quad (19)$$

where  $itr$  denotes the current iteration number.

- Step 6: stop criterion. Steps 3, 4, and 5 will be repeated until the algorithm reach the stop criterion.

#### 4.5. Phase V: Classification

A KNN classifier is used in this work. In this proposed method, the dataset is split into 60% training, 20% validation, and 20% testing.

### 5. Experiments and Results

This section thoroughly explains the performance of the proposed method (BAT) of EEG channels for stroke patient rehabilitation. Since the proposed approach is non-deterministic, the mean accuracy rate over 20 runs is computed to avoid biased results. The experiments use a Ideapad 310 Lenovo PC, China. Intel Core i7<sup>®</sup> 2.59 Ghz processor, 16 GB of RAM, and official Windows 10. The performance of the proposed method is evaluated using two measures, namely, accuracy and the number of EEG channels selected, with light shed on the stability of the algorithms by computing the best, worst, and mean accuracy. Moreover, a statistical test is adopted based on the classification accuracy of the motor/imaging EEG dataset using the sum of ranks of the metaheuristic algorithms. The proposed method is tested using three types of EEG features: time domain features, frequency domain features, and entropy domain features. Furthermore, the performance results of the proposed method are evaluated using a statistical test to show the significance of the proposed method compared with other metaheuristic algorithms.

Table 1 shows the parameters used for the selected metaheuristic algorithms that are used in this work.

#### 5.1. Time Domain Results

Table 2 presents the results of seven features in the time domain: Higuchi's fractal dimension (HFD); the Hjorth parameters Hjorth activity (HjAc), Hjorth complexity (HjComp), and Hjorth mobility (HjMo); Hurst (Hur); kurtosis (Kurt); and skewness (Skw). The accuracy and the number of EEG channels selected are two measurements to evaluate the seven features chosen for the motor/imaging EEG dataset. The evaluation metrics are classified into three categories: best, worst, and mean accuracy and no. of channels selected to evaluate the algorithms' stability.

According to Table 2, the performance results for the metaheuristic algorithms PSO, GWO, FFA, CS, and BAT with several features achieved different and remarkable accuracy concerning best, worst, and mean accuracy and the number of channels selected. For the HFD feature, the BAT algorithm achieved better accuracies of 99, 97.5, and 92.8 for best, mean, and worst accuracy and channel selection, respectively. For the HjAc feature, the BAT algorithm achieved high accuracy, 97.7, for accuracy and no. of channels selected in the best case, while PSO achieved a valuable ratio of 94.4 and 85.3 in accuracy and the number of channels selected in the mean and worst cases, respectively. For the HjComp feature, the PSO algorithm achieved an accuracy of 88.6 and 84.7 concerning mean and worst cases, while the BAT algorithm achieved the highest accuracy of 93.8 in the best case. For the HjMo feature, BAT obtained 97.8, 95.4, and 88.6 for best, mean, and worst among other metaheuristic algorithms. For the Hur feature, PSO gained high accuracies of 72.8, 65.2, and 56.6 for best, mean, and worst, respectively. For the Kurt feature, the BAT

algorithm obtained valuable accuracies of 73.2, 68.8, and 63.1 for best, mean, and worst accuracy and the number of channels selected, respectively.

Moreover, for Skw, BAT achieved high accuracies of 79.2 and 72.5 for best and mean, respectively, compared with PSO, which obtained an accuracy of 58 in the worst case of accuracy. Figure 4 shows the results of the time domain features for the convergence rate and channel distribution, comparing the BAT and PSO algorithms, which achieved the highest accuracy over the other metaheuristic algorithms, i.e., GWO, FFA, and CS. In Figure 4a, the convergence rate shows the channels and the number of iterations for the BAT and PSO algorithms. In addition, Figure 4b presents the effective and emotive channels when channels are distributed in the BAT and PSO algorithms.

**Table 2.** The performance of metaHeuristic algorithms with several feature extraction approaches for motor/imaging EEG dataset.

Feature/Algorithm			PSO	GWO	FFA	CS	BAT
<i>HFD</i>	Best	Accuracy	97.9	90.7	66.7	54.9	<b>99</b>
		No. channels	8	3	1	1	6
	Worst	Accuracy	81.5	67.4	45.1	43.2	<b>92.8</b>
		No. channels	12	6	3	2	13
	Mean	Accuracy	94.4	76.2	56.7	50.6	<b>97.5</b>
		No. channels	9	4	2	2	10
<i>HjAc</i>	Best	Accuracy	97.1	88.4	68.8	55.1	<b>97.7</b>
		No. channels	5	3	1	1	4
	Worst	Accuracy	<b>85.3</b>	70.4	41.7	42.1	77.9
		No. channels	9	5	3	2	14
	Mean	Accuracy	<b>94.4</b>	82.1	60.7	48.7	90.8
		No. channels	8	4	3	2	8
<i>HjComp</i>	Best	Accuracy	91.2	78.9	58.8	48.7	<b>93.8</b>
		No. channels	7	3	2	1	5
	Worst	Accuracy	<b>84.7</b>	58.1	47.4	40.9	74.7
		No. channels	15	6	3	2	13
	Mean	Accuracy	<b>88.6</b>	69.9	53.9	44.2	88.2
		No. channels	9	4	3	1	9
<i>HjMo</i>	Best	Accuracy	96.5	89.3	67.9	53.5	<b>97.9</b>
		No. channels	6	2	2	1	5
	Worst	Accuracy	86.4	51.8	53.9	43.8	<b>88.6</b>
		No. channels	11	6	3	2	12
	Mean	Accuracy	92.3	80.6	61.2	47.9	<b>95.4</b>
		No. channels	9	4	3	1	9
<i>Hur</i>	Best	Accuracy	<b>72.8</b>	57.9	47.2	44.1	70.1
		No. channels	4	2	1	1	5
	Worst	Accuracy	<b>56.6</b>	44.1	41.5	41.3	53.9
		No. channels	10	6	3	2	11
	Mean	Accuracy	<b>65.2</b>	51.7	44.7	42.6	64.9
		No. channels	8	4	3	2	9

Table 2. Cont.

Feature/Algorithm			PSO	GWO	FFA	CS	BAT
Kurt	Best	Accuracy	71.2	61	48.4	43.4	<b>73.2</b>
		No. channels	7	3	2	1	7
	Worst	Accuracy	56.5	48.2	43.3	40.3	<b>63.1</b>
		No. channels	12	6	3	2	12
	Mean	Accuracy	65.6	54.9	45.4	42	<b>68.8</b>
		No. channels	9	5	3	2	10
Skw	Best	Accuracy	78.7	63.7	50	44.4	<b>79.2</b>
		No. channels	4	1	2	1	3
	Worst	Accuracy	<b>58</b>	41	43.2	40.4	48.2
		No. channels	11	6	3	2	13
	Mean	Accuracy	69.6	53.3	45.9	42.3	<b>72.5</b>
		No. channels	7	4	2	2	9

5.2. Entropy Domain Results

Table 3 shows the results of the performance accuracy using seven entropy features, namely, ConFuzEn, FuzEn, impe, MFEmu, RCMFEmu, SampEn, and TsEn. Based on the accuracy and the number of selected channels for best, worst, and mean cases, these entropy features are used to compare the five metaheuristic algorithms, PSO, GWO, FFA, CS, and BAT, respectively. Compared to the other seven entropy features, the best classification performance achieved the highest accuracy using ConFuzEn with the PSO algorithm compared to the GWO, FFA, CS, and BAT algorithms. Other entropy features produced higher accuracy results with the BAT algorithm than the PSO, GWO, FFA, and CS algorithms. The BAT algorithm registered accuracies of 95.5, 95.6, 88.1, 87.2, 91.4, and 84.6 using FuzEn, impe, MFEmu, RCMFEmu, SampEn, and TsEn, respectively. Furthermore, Figure 5 presents the performance evaluation results between the BAT and PSO algorithms concerning the convergence rate and channel distribution.

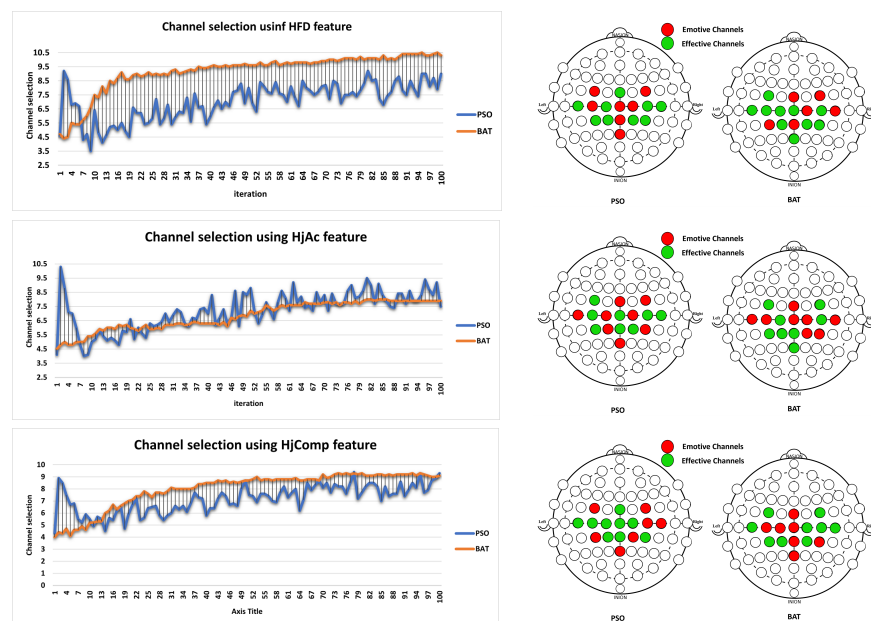


Figure 5. Cont.

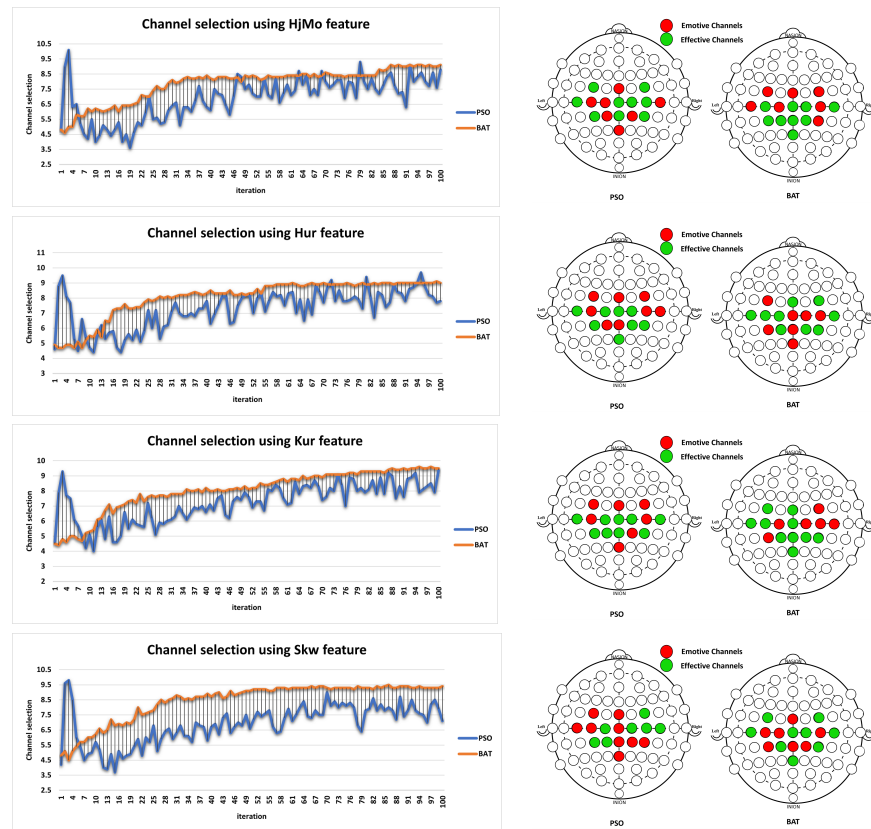


Figure 5. Convergence rate and channel distribution.

Table 3. The performance of metaHeuristic algorithms with several feature extraction approaches for motor/imaging EEG dataset.

Feature/Algorithm			PSO	GWO	FFA	CS	BAT
ConvFuzEn	Best	Accuracy	96.6	82.7	61.3	52	96.5
		No. channels	3	3	1	1	7
	Worst	Accuracy	76.4	64.7	45.5	42.5	87.1
		No. channels	11	6	3	2	14
	Mean	Accuracy	90.2	73.6	54.9	45.8	93.2
		No. channels	8	5	2	1	11
FuzEn	Best	Accuracy	93.6	81.6	60.6	49.1	95.5
		No. channels	2	4	2	1	8
	Worst	Accuracy	82.2	68.7	50.5	41.8	88.9
		No. channels	10	6	3	2	12
	Mean	Accuracy	88.6	74.4	55.7	45.5	92.1
		No. channels	7	5	3	1	10
impen	Best	Accuracy	94.7	78.6	59.3	49.8	95.6
		No. channels	5	3	2	1	7
	Worst	Accuracy	75.8	56.1	47.9	44.3	84.9
		No. channels	10	6	3	2	12
	Mean	Accuracy	85.3	69.8	52.3	46.6	90.8
		No. channels	8	5	2	2	10

Table 3. Cont.

Feature/Algorithm			PSO	GWO	FFA	CS	BAT
MFEmu	Best	Accuracy	85.2	73.6	54.3	46.8	<b>88.1</b>
		No. channels	7	3	2	1	7
	Worst	Accuracy	70.8	55.9	45.1	40.5	<b>75.5</b>
		No. channels	12	6	3	2	12
	Mean	Accuracy	80.7	66.1	49.4	44.8	<b>84</b>
		No. channels	9	5	2	2	9
RCMFEmu	Best	Accuracy	84.3	67.7	51.9	46.6	<b>87.2</b>
		No. channels	4	2	2	1	8
	Worst	Accuracy	63.7	47	44.9	41.2	<b>75.3</b>
		No. channels	12	6	3	2	13
	Mean	Accuracy	77.3	56.5	47.7	43	<b>80.3</b>
		No. channels	8	4	2	1	10
SampEn	Best	Accuracy	87.9	71.5	52.9	51.9	<b>91.4</b>
		No. channels	6	3	1	1	7
	Worst	Accuracy	75.4	53.2	42.6	40.4	<b>75.9</b>
		No. channels	10	6	3	3	14
	Mean	Accuracy	81.4	63.7	48.2	44.3	<b>83.6</b>
		No. channels	8	5	2	2	10
TsEn	Best	Accuracy	83.9	72.5	52.3	46.6	<b>84.6</b>
		No. channels	7	3	1	1	4
	Worst	Accuracy	65.9	54.4	41.2	40.2	<b>61.3</b>
		No. channels	12	7	3	2	13
	Mean	Accuracy	78.7	64.5	47.2	42.8	<b>79.8</b>
		No. channels	10	5	2	1	10

5.3. Frequency Domain Results

Based on Table 4, the frequency domain features of meanF and medF obtained high accuracies of 96.7 and 83.4 for the PSO and BAT algorithms, respectively. In the best, worst, and mean cases, meanF gained a significant accuracy relative to the medF feature on the overall accuracy results for the PSO and BAT algorithms. The best accuracy of medF was obtained at 96.7 with PSO, while the worst and mean achieved accuracies were 90.3 and 93.8 with the BAT algorithm, respectively. Moreover, the BAT algorithm scored high accuracy classification results of 83.4 and 78.4 relative to the best and worst accuracies with the feature of medF, respectively, while PSO gained an accuracy of 69.5. The convergence rate and the channel distribution are shown in Figure 6.

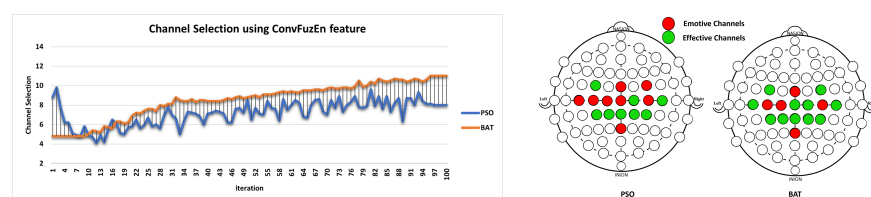


Figure 6. Cont.

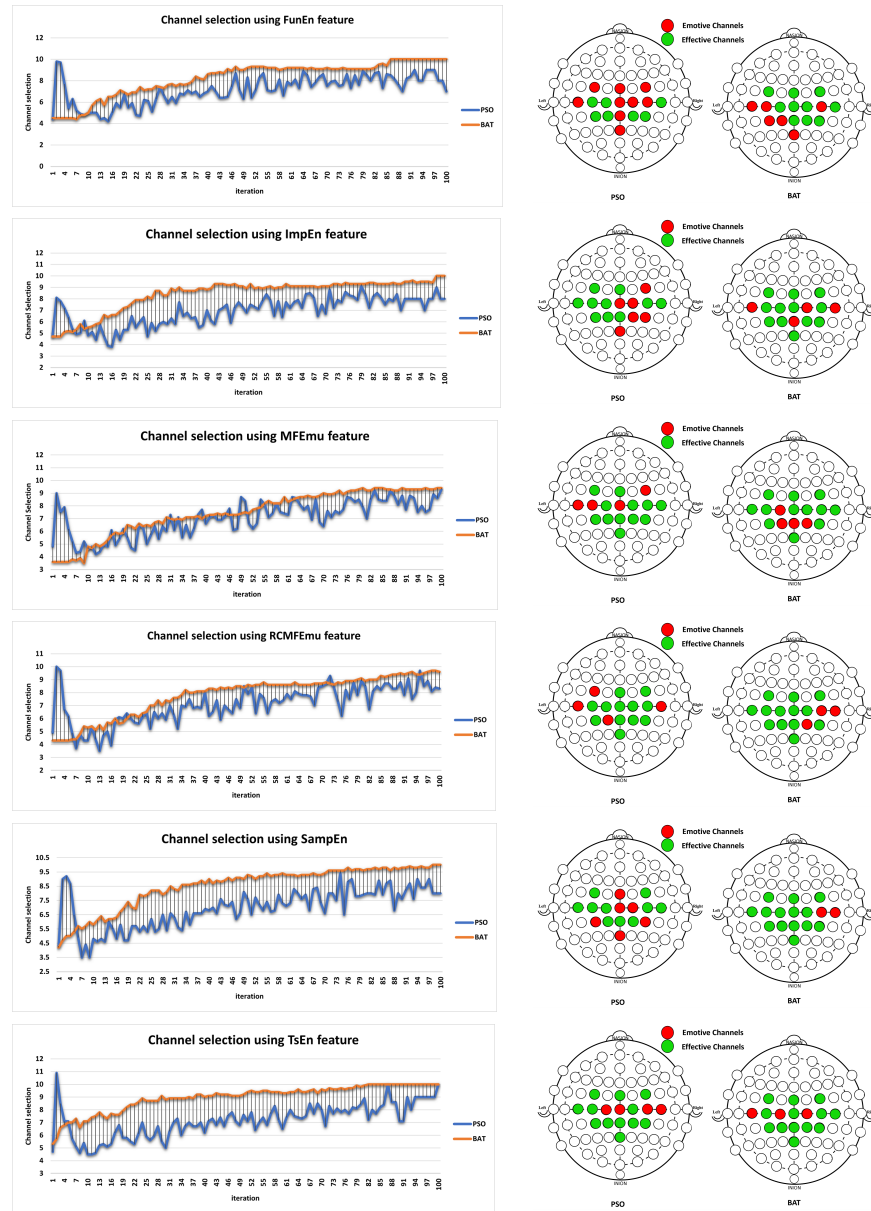


Figure 6. Convergence rate and channel distribution.

As mentioned, Table 4 shows the performance of the proposed method (BAT) compared with the PSO, GWO, FFA, and CS algorithms using frequency domain features. The BAT algorithm achieved better results than all other algorithms except in some cases in which the PSO algorithm slightly outperformed it, such as in *meanF*, where the best accuracy was 96.7 for PSO and 96.3 for BAT. However, the overall runs of the BAT algorithm achieved better results with accuracy measures equal to 93.8, 91.2, 76.4, 54, and 50 for the BAT, PSO, GWO, FFA, and CS algorithms, respectively. The convergence rate and the channel distribution are shown in Figure 7.

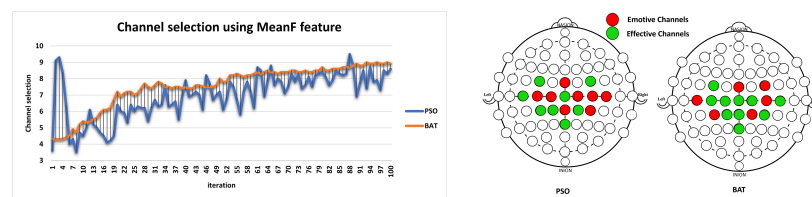


Figure 7. Cont.

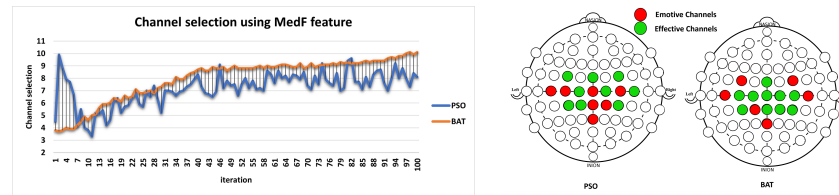


Figure 7. Convergence rate and channel distribution.

Table 4. The performance of BAT algorithm compared with several metaheuristic algorithms using frequency domain features.

Feature/Algorithm		PSO	GWO	FFA	CS	BAT
meanF	Best Accuracy	96.7	87.3	64.1	52.5	96.3
	No. channels	5	3	2	1	7
	Worst Accuracy	65.4	66	50.2	41.9	90.3
	No. channels	10	6	3	2	12
Mean	Accuracy	91.2	76.4	54	50	93.8
	No. channels	8	4	2	2	10
MedF	Best Accuracy	82.7	69.2	53.6	46.6	83.4
	No. channels	6	3	2	1	6
	Worst Accuracy	69.5	55.5	41	20	68.7
	No. channels	10	6	3	2	14
	Mean Accuracy	76.3	60.6	46.1	36.5	<b>78.4</b>
	No. channels	9	4	2	2	10

#### 5.4. Statistical Analysis Results

Before presenting our findings for the accuracy and no. of channels selected for improving the classification performance of the stroke EEG signals’ time, entropy, and frequency features analysis, we would like to examine the influence of classification accuracy in the motor/imaging EEG dataset by the adoption of the sum of ranks of the metaheuristic algorithms. In this way, the feature that improved the rank accuracy of selected channels can be identified.

As shown in Table 5, we performed the sum of ranks of the PSO, GWO, FFA, CS, and BAT metaheuristic algorithms according to the individual feature domain. In the time domain, we tested seven features. The BAT algorithm significantly improved the accuracy rank, especially in HFD and Hjac, for an accuracy rank of 99 and 97.7, respectively. Moreover, other features in the time domain, such as HjComp, HjMo, Kurt, and Skw, showed an influential impact on the classification accuracy results relative to the sum of the rank of the BAT algorithm except for the Hur feature, which had a high effect on the PSO algorithm. However, in the statistical test phase, the BAT algorithm had low summation-of-rank results among other metaheuristic algorithms.

On the other hand, the sum of ranks for the BAT algorithm showed a meaningful impact on the classification accuracy results relative to the seven features of the entropy domain except for the ConvFuzEn feature, which had a remarkable effect on the PSO algorithm with a difference of 0.1 compared with BAT concerning the sum-of-rank results in the statistical analysis. However, the BAT algorithm had low summation-of-rank results in the statistical test phase among the other metaheuristic algorithms.

However, in the classification accuracy results from the frequency domain features, meanF showed a salient ameliorating effect on the accuracy with the PSO algorithm relative to the accuracy rank 96.7 compared with the medF feature, which had an 83.4 accuracy

rank with the BAT algorithm. Moreover, the BAT and PSO algorithms had low summation-of-rank results among other metaheuristic algorithms.

**Table 5.** The sum of ranks of metaHeuristic algorithms based on classification accuracy on motor/imaging EEG dataset.

Feature/Algorithm		PSO	GWO	FFA	CS	BAT
HFD	Accuracy	97.9	90.7	66.7	54.9	99
	Rank	2	3	4	5	1
HjAc	Accuracy	97.1	88.4	68.8	55.1	97.7
	Rank	2	3	4	5	1
HjComp	Accuracy	91.2	78.9	58.8	48.7	93.8
	Rank	2	3	4	5	1
TDF HjMo	Accuracy	96.5	89.3	67.9	53.5	97.9
	Rank	2	3	4	5	1
Hur	Accuracy	72.8	57.9	47.2	44.1	70.1
	Rank	1	3	4	5	2
Kur	Accuracy	71.2	61	48.4	43.4	73.2
	Rank	2	3	4	5	1
Skw	Accuracy	78.7	63.7	50	44.4	<b>79.2</b>
	Rank	2	3	4	5	1
Summation of Ranks		13	21	28	35	<b>8</b>
meanF	Accuracy	96.7	87.3	64.1	52.5	96.3
	Rank	1	3	4	5	2
FDF MedF	Accuracy	82.7	69.2	53.6	46.6	<b>83.4</b>
	Rank	2	3	4	5	1
Summation of Ranks		3	6	8	10	3
ConvFuzEn	Accuracy	96.6	82.7	61.3	52	96.5
	Rank	1	3	4	5	2
FuzEn	Accuracy	93.6	81.6	60.6	49.1	95.5
	Rank	2	3	4	5	1
impen	Accuracy	94.7	78.6	59.3	49.8	95.6
	Rank	2	3	4	5	1
EDF MFEmu	Accuracy	85.2	73.6	54.3	46.8	88.1
	Rank	2	3	4	5	1
RCMFEmu	Accuracy	84.3	67.7	51.9	46.6	<b>87.2</b>
	Rank	2	3	4	5	1
SampEn	Accuracy	87.9	71.5	52.9	51.9	91.4
	Rank	2	3	4	5	1
TsEn	Accuracy	83.9	72.5	52.3	46.6	84.6
	Rank	2	3	4	5	1
Summation of Ranks		13	21	28	35	8

Figure 8 shows the results of the speed of metaheuristic algorithms in seconds.

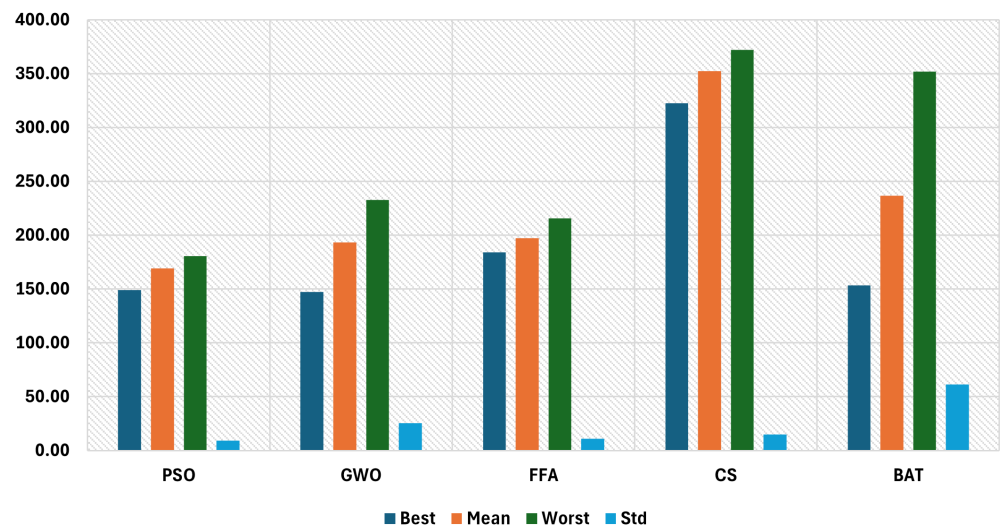


**Figure 8.** Speed of metaheuristic algorithms in seconds.

### 5.5. Results Discussion

This research aims to choose the most relevant EEG channels that produce an effective accuracy rate for stroke patient rehabilitation by using a binary bat algorithm-based optimization technique to optimize TEF characteristics. To further improve the classification performance of stroke EEG signals, three types of features (namely, time, entropy, and frequency domain features) were used as the baseline for the classification task. Two measurements were applied to evaluate the performance of the proposed method, accuracy and no. of EEG channels selected. Furthermore, we adopted a statistical test using the sum of the ranks for the motor/imaging EEG dataset to examine the influence of the classification accuracy and the significance of the suggested method compared with state-of-the-art metaheuristic algorithms such as PSO, GWO, FFA, and CS. Firstly, the accuracy and the no. of EEG channels selected were evaluated by computing the best, worst, and mean accuracy values to capture the stability of the implemented algorithm. In the time domain, seven features were tested, and the HFD feature had the most significant influence on the improvement of the classification task in the BAT optimizer among other optimization algorithms for the best, mean, and worst cases of accuracy and the no. of channels selected, respectively, based on a kNN classifier. In addition, the BAT results outperformed in the testing values for the best accuracy case compared with PSO, which had the highest results compared with the GWO, FFA, and CS algorithms in the HjAc and HjComp features. Moreover, the results for the BAT optimizer registered high best, mean, and worst accuracy values and the no. of channels selected, respectively, with the HFD, HjMo, and Kurt features, respectively, while PSO had the most significant influence on the improvement of the classification task compared with BAT with the Hur feature based on best, mean, and worst accuracy and the no. of channels selected, respectively. For the best-case values, the BAT optimizer outperformed in the valuable and highest values among PSO and the other metaheuristic algorithms with the six features of HFD, HjAc, HjComp, HjMo, Kurt, and Skw, respectively (see Table 2). Furthermore, according to the results of the performance accuracy using seven entropy features based on the KNN classifier, the best classification performance was achieved with the highest accuracy using ConFuzEn with the PSO algorithm compared to the GWO, FFA, CS, and BAT algorithms. Other entropy features produced higher accuracy results with the BAT algorithm than the PSO, GWO, FFA, and CS algorithms according to the best, mean, and worst accuracy values and the no. of channels selected, respectively. The BAT algorithm registered best-case accuracy values of 95.5, 95.6, 88.1, 87.2, 91.4, and 84.6 using the FuzEn, impe, MFEmu, RCMFEmu, SampEn, and TsEn features, respectively, while PSO outperformed BAT with accuracy result values for the ConvFuzEn feature for the KNN classifier (see Table 3).

The BAT and PSO algorithms obtained high accuracies of 96.7 and 83.4, respectively, compared with other algorithms in the literature for meanF and medF frequency domain features. The BAT algorithm scored high accuracy classification results of 83.4 and 78.4 relative to the best and worst accuracies with the feature of medF, respectively, while PSO gained an accuracy of 69.5; furthermore, the PSO and BAT algorithms gained significantly in accuracy relative to the medF feature on the overall accuracy results in the best, worst, and mean accuracy cases. Based on the classification results on the basis of the features from the three different domains types, the BAT and PSO algorithms exerted significant impacts on the classification performance compared with the results of the GWO, FFA, and CS optimization algorithms concerning the accuracy and the no. of channels selected, respectively. Hence, they demonstrate a significant improvement in the average accuracy relative to the classification result on the basis of the individual feature domains, as can be seen in Figure 5, which explains the comparison between the convergence rate and channel distribution for the BAT and PSO algorithms.

Second, we examined the influence of classification accuracy on the motor/imaging EEG dataset using the adopted sum of ranks of metaheuristic algorithms. Thus, the feature that improved the rank accuracy of the selected channels can be identified. The BAT algorithm significantly improved the accuracy rank, especially in the HFD and Hjac features, with an accuracy rank of 99 and 97.7, respectively, compared with the PSO, GWO, FFA, and CS algorithms according to the sum-of-ranks results with respect to the time domain. Furthermore, features such as HjComp, HjMo, Kurt, and Skw showed an influential impact on the classification accuracy results relative to the sum of the rank of the BAT algorithm except for the Hur feature, which had a high effect on the PSO algorithm. However, in the statistical test phase, the BAT algorithm had low summation-of-rank results among the other metaheuristic algorithms. Further, the BAT algorithm showed a meaningful impact on the classification accuracy results for the sum of ranks relative to the seven features of the entropy domain except for the ConvFuzEn feature, which had a remarkable effect on the PSO algorithm with a difference of 0.1 compared with BAT concerning the sum-of-rank results in the statistical analysis. However, in the statistical test phase, the BAT algorithm had a low summation-of-rank results among the other metaheuristic algorithms. Moreover, the BAT and PSO algorithms had low summation-of-rank results among the other metaheuristic algorithms in the frequency domain features. The meanF feature showed a salient ameliorating effect on the accuracy with the PSO algorithm relative to the accuracy rank of 96.7 compared with the medF feature, which had an 83.4 accuracy rank with the BAT algorithm.

## 6. Conclusions and Future Work

This paper proposes a new method for EEG channel selection based on an optimization algorithm called the BAT-inspired algorithm. The main purpose of the proposed algorithm is to select the most relevant EEG channels that can provide a higher accuracy rate for stroke patient rehabilitation.

The proposed method was tested using a standard EEG dataset collected from eight poststroke patients with hemiparesis of the upper extremities. The EEG data were captured using EEG caps with 16 active electrodes from g.Nautilus PRO, g.tec medical engineering GmbH, Austria.

The proposed method used several EEG feature extraction methods such as the time domain, frequency domain, and entropy domain. In addition, the proposed method (BAT) was compared with four metaheuristic algorithms, namely, particle swarm optimization (PSO), grey wolf optimizer (GWO), cuckoo search (CS), and firefly algorithm (FFA). The performance of the proposed method was evaluated using the accuracy rate and the number of channels selected. The proposed method achieved the best results over all the feature extraction methods and showed a significant improvement using a standard statistical analysis test called the summation of ranks test.

Finally, the proposed method succeeded in reducing the number of EEG channels to less than half while maintaining the accuracy rate.

Regarding future works, the proposed method suffers from some problems; for example, the proposed method is unable to generate new solutions that have the ability to increase accuracy (i.e., stuck in local minima). For that, the proposed method will need to be improved to overcome this problem by modifying the mechanism of the BAT algorithm or hybridizing the BAT algorithm with another metaheuristic algorithm to be able to find the optimal solution. Regarding the second problem, the current version of the BAT algorithm focuses on finding the optimal solution that provides the highest accuracy rate and does not consider the number of EEG channels in the objective function. Therefore, in future work, we will work on the proposed multiobjective BAT version using the highest accuracy and the lowest number of EEG channels simultaneously.

**Author Contributions:** Conceptualization, M.A.A.-B., Z.A.A.A. and N.K.A.-Q.; methodology, M.A.A.-B., Z.A.A.A. and N.K.A.-Q.; software, M.A.A.-B. and Z.A.A.A.; validation, M.A.A.-B. and S.N.M.; investigation, M.A.A.-B. and Z.A.A.A.; resources, M.A.A.-B., Z.A.A.A. and C.G.; writing—original draft, M.A.A.-B., Z.A.A.A., N.K.A.-Q., S.N.M., N.S.A. and C.G.; Visualization, M.A.A.-B., Z.A.A.A., S.N.M., N.S.A. and C.G. All authors have read and agreed to the published version of the manuscript.

**Funding:** This work was supported by the Deanship of Research and Graduate Studies (DRG) at Ajman University, Ajman, UAE (Grant No. 2022-IRG-ENIT-7).

**Data Availability Statement:** Data are contained within the article.

**Conflicts of Interest:** Author Christoph Guger was employed by the g.tec medical engineering GmbH. The remaining authors declare that the research was conducted in the absence of any commercial or financial relationships that could be construed as a potential conflict of interest.

## References

- Li, F.; Fan, Y.; Zhang, X.; Wang, C.; Hu, F.; Jia, W.; Hui, H. Multi-Feature Fusion Method Based on EEG Signal and its Application in Stroke Classification. *J. Med. Syst.* **2020**, *44*, 39. [[CrossRef](#)]
- Khairunizam, W.; Yean, C.W.; Murugappan, M.; Junoh, A.K.; Razlan, Z.M.; Shahrman, A.; Mustafa, W.A.W.; Ibrahim, Z.; Nurhafizah, S. An Experimental Framework for Assessing Emotions of Stroke Patients using Electroencephalogram (EEG). *J. Phys. Conf. Ser.* **2020**, *1529*, 052072. [[CrossRef](#)]
- Carino-Escobar, R.I.; Carrillo-Mora, P.; Valdés-Cristerna, R.; Rodriguez-Barragan, M.A.; Hernandez-Arenas, C.; Quinzaños-Fresnedo, J.; Galicia-Alvarado, M.A.; Cantillo-Negrete, J. Longitudinal analysis of stroke patients' brain rhythms during an intervention with a brain-computer interface. *Neural Plast.* **2019**, *2019*. [[CrossRef](#)] [[PubMed](#)]
- Grefkes, C.; Fink, G.R. Connectivity-based approaches in stroke and recovery of function. *Lancet Neurol.* **2014**, *13*, 206–216. [[CrossRef](#)]
- Hachinski, V.; Donnan, G.A.; Gorelick, P.B.; Hacke, W.; Cramer, S.C.; Kaste, M.; Fisher, M.; Brainin, M.; Buchan, A.M.; Lo, E.H.; et al. Stroke: Working toward a prioritized world agenda. *Stroke* **2010**, *41*, 1084–1099. [[CrossRef](#)] [[PubMed](#)]
- Gao, W.; Cui, Z.; Yu, Y.; Mao, J.; Xu, J.; Ji, L.; Kan, X.; Shen, X.; Li, X.; Zhu, S.; et al. Application of a Brain–Computer Interface System with Visual and Motor Feedback in Limb and Brain Functional Rehabilitation after Stroke: Case Report. *Brain Sci.* **2022**, *12*, 1083. [[CrossRef](#)]
- Jin, J.; Qu, T.; Xu, R.; Wang, X.; Cichocki, A. Motor Imagery EEG Classification Based on Riemannian Sparse Optimization and Dempster-Shafer Fusion of Multi-Time-Frequency Patterns. *IEEE Trans. Neural Syst. Rehabil. Eng.* **2022**, *31*, 58–67. [[CrossRef](#)]
- Al-Qazzaz, N.K.; Alyasseri, Z.A.A.; Abdulkareem, K.H.; Ali, N.S.; Al-Mhiqani, M.N.; Guger, C. EEG feature fusion for motor imagery: A new robust framework towards stroke patients rehabilitation. *Comput. Biol. Med.* **2021**, *137*, 104799. [[CrossRef](#)]
- Al-Timemy, A.H.; Bugmann, G.; Outram, N.; Escudero, J. Reduction in classification errors for myoelectric control of hand movements with independent component analysis. In Proceedings of the The 5th International Conference on Information Technology, ICIT, Bali, Indonesia, 26–28 October 2011; Volume 2011.
- Al-Qazzaz, N.K.; Ali, S.H.B.M.; Ahmad, S.A.; Escudero, J. Optimal EEG Channel Selection for Vascular Dementia Identification Using Improved Binary Gravitation Search Algorithm. In Proceedings of the International Conference for Innovation in Biomedical Engineering and Life Sciences, Penang, Malaysia, 10–13 December 2017; pp. 125–130.
- Al-Qazzaz, N.K.; Sabir, M.K.; Ali, S.H.B.M.; Ahmad, S.A.; Grammer, K. Multichannel optimization with hybrid spectral-entropy markers for gender identification enhancement of emotional-based EEGs. *IEEE Access* **2021**, *9*, 107059–107078. [[CrossRef](#)]
- Velasco, I.; Sipols, A.; De Blas, C.S.; Pastor, L.; Bayona, S. Motor imagery EEG signal classification with a multivariate time series approach. *Biomed. Eng. OnLine* **2023**, *22*, 29. [[CrossRef](#)]

13. Jouzizadeh, M. EEG-Assessed Network and Signal Variability Features in Males and Females during a Visuospatial Task. Ph.D. Thesis, Université d'Ottawa/University of Ottawa, Ottawa, ON, Canada, 2024.
14. Al-Qazzaz, N.K.; Sabir, M.K.; Ali, S.; Ahmad, S.A.; Grammer, K. Effective EEG channels for emotion identification over the brain regions using differential evolution algorithm. In Proceedings of the 2019 41st Annual International Conference of the IEEE Engineering in Medicine and Biology Society (EMBC), Berlin, Germany, 23–27 July 2019; pp. 4703–4706.
15. Dornhege, G.; Millán, J.d.R.; Hinterberger, T.; McFarland, D.J.; Muller, K.R. *Toward Brain-Computer Interfacing*; MIT Press: Cambridge, MA, USA, 2007; Volume 63.
16. Kingphai, K.; Moshfeghi, Y. On channel selection for EEG-based mental workload classification. In Proceedings of the International Conference on Machine Learning, Optimization, and Data Science, Grasmere, UK, 22–26 September 2023; pp. 403–417.
17. Liu, T.; Wu, Y.; Ye, A.; Cao, L.; Cao, Y. Two-stage sparse multi-objective evolutionary algorithm for channel selection optimization in BCIs. *Front. Hum. Neurosci.* **2024**, *18*, 1400077. [[CrossRef](#)] [[PubMed](#)]
18. Soleimani, B.; Dallasta, I.; Das, P.; Kulasingham, J.P.; Girgenti, S.; Simon, J.Z.; Babadi, B.; Marsh, E.B. Altered directional functional connectivity underlies post-stroke cognitive recovery. *Brain Commun.* **2023**, *5*, fcad149. [[CrossRef](#)] [[PubMed](#)]
19. Seguin, C.; Sporns, O.; Zalesky, A. Brain network communication: Concepts, models and applications. *Nat. Rev. Neurosci.* **2023**, *24*, 557–574. [[CrossRef](#)] [[PubMed](#)]
20. Mang, J.; Xu, Z.; Qi, Y.; Zhang, T. Favoring the cognitive-motor process in the closed-loop of BCI mediated post stroke motor function recovery: Challenges and approaches. *Front. Neurorobotics* **2023**, *17*, 1271967. [[CrossRef](#)] [[PubMed](#)]
21. Nunez, P.L.; Srinivasan, R.; Westdorp, A.F.; Wijesinghe, R.S.; Tucker, D.M.; Silberstein, R.B.; Cadusch, P.J. EEG coherency: I: Statistics, reference electrode, volume conduction, Laplacians, cortical imaging, and interpretation at multiple scales. *Electroencephalogr. Clin. Neurophysiol.* **1997**, *103*, 499–515. [[CrossRef](#)] [[PubMed](#)]
22. Al-Qazzaz, N.K.; Hamid Bin Mohd Ali, S.; Ahmad, S.A.; Islam, M.S.; Escudero, J. Automatic artifact removal in EEG of normal and demented individuals using ICA–WT during working memory tasks. *Sensors* **2017**, *17*, 1326. [[CrossRef](#)] [[PubMed](#)]
23. Al-Qazzaz, N.K.; Ali, S.H.B.M.; Ahmad, S.A.; Islam, M.S.; Escudero, J. Discrimination of stroke-related mild cognitive impairment and vascular dementia using EEG signal analysis. *Med. Biol. Eng. Comput.* **2018**, *56*, 137–157. [[CrossRef](#)] [[PubMed](#)]
24. Zhang, Y.; Nam, C.S.; Zhou, G.; Jin, J.; Wang, X.; Cichocki, A. Temporally constrained sparse group spatial patterns for motor imagery BCI. *IEEE Trans. Cybern.* **2018**, *49*, 3322–3332. [[CrossRef](#)] [[PubMed](#)]
25. Chaudhary, S.; Taran, S.; Bajaj, V.; Siuly, S. A flexible analytic wavelet transform based approach for motor-imagery tasks classification in BCI applications. *Comput. Methods Programs Biomed.* **2020**, *187*, 105325. [[CrossRef](#)]
26. Duan, L.; Hongxin, Z.; Khan, M.S.; Fang, M. Recognition of motor imagery tasks for BCI using CSP and chaotic PSO twin SVM. *J. China Univ. Posts Telecommun.* **2017**, *24*, 83–90. [[CrossRef](#)]
27. Alotaiby, T.; Abd El-Samie, F.E.; Alshebeili, S.A.; Ahmad, I. A review of channel selection algorithms for EEG signal processing. *EURASIP J. Adv. Signal Process.* **2015**, *2015*, 66. [[CrossRef](#)]
28. He, L.; Yu, Z.; Gu, Z.; Li, Y. Bhattacharyya bound based channel selection for classification of motor imageries in EEG signals. In Proceedings of the 2009 Chinese Control and Decision Conference, Guilin, China, 17–19 June 2009; pp. 2353–2356.
29. Tam, W.K.; Ke, Z.; Tong, K.Y. Performance of common spatial pattern under a smaller set of EEG electrodes in brain-computer interface on chronic stroke patients: A multi-session dataset study. In Proceedings of the 2011 annual International Conference of the IEEE Engineering in Medicine and Biology Society, Boston, MA, USA, 30 August–3 September 2011; pp. 6344–6347.
30. Gómez-López, J.C.; Escobar, J.J.; Díaz, A.F.; Damas, M.; Gil-Montoya, F.; González, J. Boosting the convergence of a GA-based wrapper for feature selection problems on high-dimensional data. In Proceedings of the Genetic and Evolutionary Computation Conference Companion, Boston, MA, USA, 9–13 July 2022; pp. 431–434.
31. Shen, C.; Zhang, K. Two-stage improved Grey Wolf optimization algorithm for feature selection on high-dimensional classification. *Complex Intell. Syst.* **2022**, *8*, 2769–2789. [[CrossRef](#)]
32. Tiwari, A.; Chaturvedi, A. Automatic EEG channel selection for multiclass brain-computer interface classification using multiobjective improved firefly algorithm. *Multimed. Tools Appl.* **2023**, *82*, 5405–5433. [[CrossRef](#)]
33. Millán, J.d.R.; Franzé, M.; Mouriño, J.; Cincotti, F.; Babiloni, F. Relevant EEG features for the classification of spontaneous motor-related tasks. *Biol. Cybern.* **2002**, *86*, 89–95. [[CrossRef](#)] [[PubMed](#)]
34. Martínez-Cagigal, V.; Santamaría-Vázquez, E.; Hornero, R. Brain-computer interface channel selection optimization using meta-heuristics and evolutionary algorithms. *Appl. Soft Comput.* **2022**, *115*, 108176. [[CrossRef](#)]
35. Gaur, P.; Gupta, H.; Chowdhury, A.; McCreddie, K.; Pachori, R.B.; Wang, H. A sliding window common spatial pattern for enhancing motor imagery classification in EEG-BCI. *IEEE Trans. Instrum. Meas.* **2021**, *70*, 4002709. [[CrossRef](#)]
36. Shi, B.; Wang, Q.; Yin, S.; Yue, Z.; Huai, Y.; Wang, J. A binary harmony search algorithm as channel selection method for motor imagery-based BCI. *Neurocomputing* **2021**, *443*, 12–25. [[CrossRef](#)]
37. Ghaemi, A.; Rashedi, E.; Pourrahimi, A.M.; Kamandar, M.; Rahdari, F. Automatic channel selection in EEG signals for classification of left or right hand movement in Brain Computer Interfaces using improved binary gravitation search algorithm. *Biomed. Signal Process. Control* **2017**, *33*, 109–118. [[CrossRef](#)]
38. Lotte, F.; Congedo, M.; Lécuyer, A.; Lamarche, F.; Arnaldi, B. A review of classification algorithms for EEG-based brain-computer interfaces. *J. Neural Eng.* **2007**, *4*, R1. [[CrossRef](#)]
39. Hassan, M.M.; Alam, M.G.R.; Uddin, M.Z.; Huda, S.; Almgren, A.; Fortino, G. Human emotion recognition using deep belief network architecture. *Inf. Fusion* **2019**, *51*, 10–18. [[CrossRef](#)]

40. Khosla, A.; Khandnor, P.; Chand, T. A comparative analysis of signal processing and classification methods for different applications based on EEG signals. *Biocybern. Biomed. Eng.* **2020**, *40*, 649–690. [[CrossRef](#)]
41. Altan, G.; Kutlu, Y.; Allahverdi, N. Deep belief networks based brain activity classification using EEG from slow cortical potentials in stroke. *Int. J. Appl. Math. Electron. Comput.* **2016**, *4*, 205–210. [[CrossRef](#)]
42. García-Laencina, P.J.; Rodríguez-Bermudez, G.; Roca-Dorda, J. Exploring dimensionality reduction of EEG features in motor imagery task classification. *Expert Syst. Appl.* **2014**, *41*, 5285–5295. [[CrossRef](#)]
43. Aler, R.; Galván, I.M. Optimizing the number of electrodes and spatial filters for Brain–Computer Interfaces by means of an evolutionary multi-objective approach. *Expert Syst. Appl.* **2015**, *42*, 6215–6223. [[CrossRef](#)]
44. Lal, T.N.; Schroder, M.; Hinterberger, T.; Weston, J.; Bogdan, M.; Birbaumer, N.; Scholkopf, B. Support vector channel selection in BCI. *IEEE Trans. Biomed. Eng.* **2004**, *51*, 1003–1010. [[CrossRef](#)] [[PubMed](#)]
45. Rakotomamonjy, A.; Guigue, V. BCI competition III: Dataset II-ensemble of SVMs for BCI P300 speller. *IEEE Trans. Biomed. Eng.* **2008**, *55*, 1147–1154. [[CrossRef](#)] [[PubMed](#)]
46. Tan, P.; Wang, X.; Wang, Y. Dimensionality reduction in evolutionary algorithms-based feature selection for motor imagery brain-computer interface. *Swarm Evol. Comput.* **2020**, *52*, 100597. [[CrossRef](#)]
47. Tsai, C.F.; Eberle, W.; Chu, C.Y. Genetic algorithms in feature and instance selection. *Knowl.-Based Syst.* **2013**, *39*, 240–247. [[CrossRef](#)]
48. Udhaya Kumar, S.; Hannah Inbarani, H. PSO-based feature selection and neighborhood rough set-based classification for BCI multiclass motor imagery task. *Neural Comput. Appl.* **2017**, *28*, 3239–3258. [[CrossRef](#)]
49. Baig, M.Z.; Aslam, N.; Shum, H.P.; Zhang, L. Differential evolution algorithm as a tool for optimal feature subset selection in motor imagery EEG. *Expert Syst. Appl.* **2017**, *90*, 184–195. [[CrossRef](#)]
50. Atyabi, A.; Luerssen, M.; Fitzgibbon, S.; Powers, D.M. Evolutionary feature selection and electrode reduction for EEG classification. In Proceedings of the 2012 IEEE Congress on Evolutionary Computation, Brisbane, QLD, Australia, 10–15 June 2012; pp. 1–8.
51. Nakisa, B.; Rastgoo, M.N.; Tjondronegoro, D.; Chandran, V. Evolutionary computation algorithms for feature selection of EEG-based emotion recognition using mobile sensors. *Expert Syst. Appl.* **2018**, *93*, 143–155. [[CrossRef](#)]
52. Al-Qazzaz, N.K.; Ali, S.H.M.; Ahmad, S.A. Differential Evolution Based Channel Selection Algorithm on EEG Signal for Early Detection of Vascular Dementia among Stroke Survivors. In Proceedings of the 2018 IEEE-EMBS Conference on Biomedical Engineering and Sciences (IECBES), Sarawak, Malaysia, 3–6 December 2018; pp. 239–244.
53. Alyasseri, Z.A.A.; Khader, A.T.; Al-Betar, M.A.; Joao, P.P.; Osama, A.A. EEG-based Person Authentication Using Multi-objective Flower Pollination Algorithm. In Proceedings of the Evolutionary Computation (CEC), Rio de Janeiro, Brazil, 8–13 July 2018; pp. 15–22.
54. Yang, X.S. A new metaheuristic bat-inspired algorithm. In *Nature Inspired Cooperative Strategies for Optimization (NICSO 2010)*; Springer: Berlin/Heidelberg, Germany, 2010; pp. 65–74.
55. Hyvarinen, A. Fast and robust fixed-point algorithms for independent component analysis. *IEEE Trans. Neural Netw.* **1999**, *10*, 626–634. [[CrossRef](#)] [[PubMed](#)]
56. Escudero, J.; Hornero, R.; Abásolo, D.; Fernández, A. Blind source separation to enhance spectral and non-linear features of magnetoencephalogram recordings. Application to Alzheimer’s disease. *Med. Eng. Phys.* **2009**, *31*, 872–879. [[CrossRef](#)] [[PubMed](#)]
57. James, C.J.; Hesse, C.W. Independent component analysis for biomedical signals. *Physiol. Meas.* **2005**, *26*, R15. [[CrossRef](#)] [[PubMed](#)]
58. Al-Qazzaz, N.K.; Hamid Bin Mohd Ali, S.; Ahmad, S.A.; Islam, M.S.; Escudero, J. Selection of mother wavelet functions for multi-channel EEG signal analysis during a working memory task. *Sensors* **2015**, *15*, 29015–29035. [[CrossRef](#)] [[PubMed](#)]
59. Escudero, J.; Hornero, R.; Abásolo, D.; Fernández, A. Quantitative evaluation of artifact removal in real magnetoencephalogram signals with blind source separation. *Ann. Biomed. Eng.* **2011**, *39*, 2274–2286. [[CrossRef](#)] [[PubMed](#)]
60. Barbati, G.; Porcaro, C.; Zappasodi, F.; Rossini, P.M.; Tecchio, F. Optimization of an independent component analysis approach for artifact identification and removal in magnetoencephalographic signals. *Clin. Neurophysiol.* **2004**, *115*, 1220–1232. [[CrossRef](#)]
61. Mammone, N.; La Foresta, F.; Morabito, F.C. Automatic artifact rejection from multichannel scalp EEG by wavelet ICA. *IEEE Sens. J.* **2011**, *12*, 533–542. [[CrossRef](#)]

**Disclaimer/Publisher’s Note:** The statements, opinions and data contained in all publications are solely those of the individual author(s) and contributor(s) and not of MDPI and/or the editor(s). MDPI and/or the editor(s) disclaim responsibility for any injury to people or property resulting from any ideas, methods, instructions or products referred to in the content.